

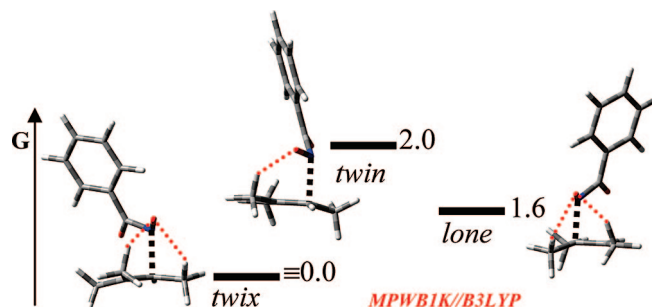
The Remarkable Cis Effect in the Ene Reactions of Nitrosocarbonyl Intermediates

Paolo Quadrelli,^{*,†} Silvano Romano,[‡] Andrea Piccanello,[†] and Pierluigi Caramella^{*,†}

Dipartimento di Chimica Organica and Unità di Ricerca CNISM e Dipartimento di Fisica "A. Volta",
Università degli Studi di Pavia, Via Bassi 6, 27100 - Pavia, Italy

paolo.quadrelli@unipv.it; pierluigi.caramella@unipv.it

Received July 24, 2008



Nitrosocarbonyls are fleeting and highly reactive intermediates that undergo ene reactions in a two-step fashion. The addition steps are rate and product determining and lead to polarized diradicals that readily enter the H-abstraction step yielding the ene products. The addition TSs are reached early, and the stabilizing CH \cdots O contacts drive the reactions to the cis adducts. B3LYP calculations alone do not describe the correct ordering of addition TSs in the ene reaction with trimethylethylene and (*E*)- and (*Z*)-3-methyl-2-penten-2-ones. Only at the MPWB1K level of treatment, medium-range noncovalent interactions are successfully recovered, accounting satisfactorily for the experimental selectivities. The more stable and isolable ArNOs exhibit late addition TSs, and distortion energies become dominant driving the reaction exclusively to the Markovnikov adducts.

Nitrosocarbonyls **1** (RCO–NO) are an exceptionally reactive species discovered by Kirby, at the beginning of the 1970s, and are traditionally generated by periodate oxidation of hydroxamic acids **2**.¹ These fleeting intermediates are versatile synthetic tools that gained wide acceptance as powerful dienophiles in hetero-Diels–Alder (HDA) cycloadditions. The synthetic potential of their HDA cycloadducts **3** can be further manipulated through additions to the double bond, cleavage of the N–O bond, and/or detachment of the acyl substituents (Scheme 1).²

Since the pioneering work by Kirby, other methods have been proposed for the in situ preparation of nitrosocarbonyls. Apart from the oxidation of hydroxamic acids with more soluble tetraalkylammonium periodate salts, other oxidative conditions have been developed,³ as well as transition metal catalyzed⁴ and PhI(OAc)₂ oxidations.⁵ Thermal cycloreversion of the HDA adducts **3** offers an alternative source of these intermediates which can be trapped with different dienes. On using the latter approach, Keck showed that the nitrosocarbonyl intermediates thermally liberated from their HDA adducts with 9,10-dimethylantracene in refluxing benzene behave as active enophiles with various olefins in an ene addition affording the adducts **4**.⁶ The oxidative generation, in fact, is not compatible

[†] Dipartimento di Chimica Organica.

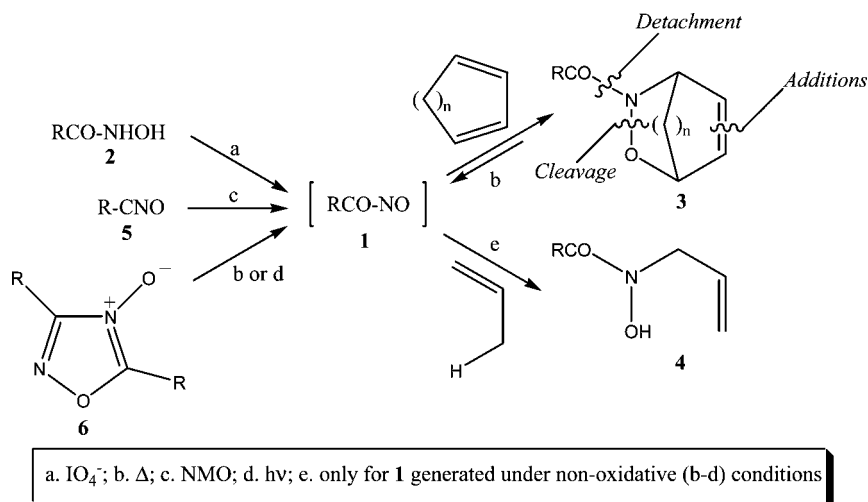
[‡] Unità di Ricerca CNISM e Dipartimento di Fisica "A. Volta".

(1) Kirby, G. W. *Chem. Soc. Rev.* **1977**, *6*, 1–24.

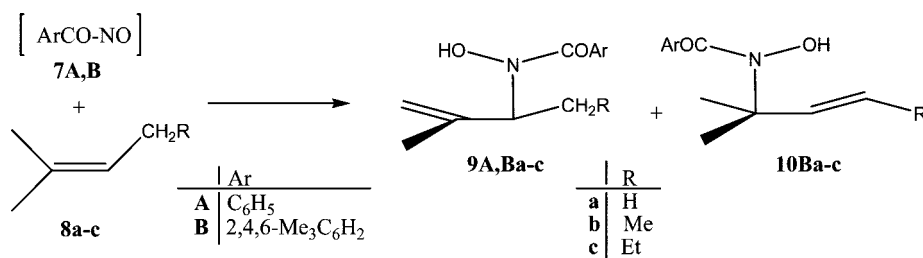
(2) (a) Vogt, P. F.; Miller, M. J. *Tetrahedron* **1998**, *54*, 1317–1348. (b) Boger, L.; Weinreb, S. M. *Hetero Diels-Alder Methodology in Organic Synthesis*; Academic Press: San Diego, CA, 1987. (c) Miller, A.; Procter, G. *Tetrahedron Lett.* **1990**, *31*, 1043–1046. (d) Kirby, G. W.; Nazeer, M. J. *Chem. Soc., Perkin Trans. 1* **1993**, 1397–1402. (e) Gouverneur, V.; McCarthy, S. J.; Mineur, C.; Belotti, D.; Dive, G.; Ghosez, L. *Tetrahedron* **1998**, *54*, 10537–10554. (f) Calvet, G.; Dussaussois, M.; Blanchard, N.; Kouklovsky, C. *Org. Lett.* **2004**, *6*, 2449–2451, and references therein. (g) Iwasa, S.; Fakhruddin, A.; Nishiyama, H. *Mini-Rev. Org. Chem.* **2005**, *2*, 157–175.

(3) (a) Surman, M. D.; Mulvihill, M. J.; Miller, M. J. *J. Org. Chem.* **2002**, *67*, 4115–4121. (b) Surman, M. D.; Mulvihill, M. J.; Miller, M. J. *Tetrahedron Lett.* **2002**, *43*, 1131–1134. (c) Ware, R. W., Jr.; Day, C. S.; King, S. B. *J. Org. Chem.* **2002**, *67*, 6174–6180. (d) Chow, C. P.; Shea, K. J.; Sparks, S. M. *Org. Lett.* **2002**, *4*, 2637–2640. (e) Momiyama, N.; Yamamoto, H. *Org. Lett.* **2002**, *4*, 3579–3582. (f) Sato, T.; Aoyagi, S.; Kibayashi, C. *Org. Lett.* **2003**, *5*, 3839–3842. (g) Jiang, M. X.-W.; Warshakoon, N. C.; Miller, M. J. *J. Org. Chem.* **2005**, *70*, 2824–2827. (h) Bodnar, B. S.; Miller, M. J. *J. Org. Chem.* **2007**, *72*, 3929–3932.

SCHEME 1



SCHEME 2



with the ene reaction since it degrades the formed adducts **4** by further oxidation.

Recently, we developed two alternative entries to nitroso carbonyls through the mild oxidation of nitrile oxides **5** with *N*-methylmorpholine-*N*-oxide (NMO)⁷ and the clean photolysis and thermolysis of 1,2,4-oxadiazole-4-oxides **6**.⁸ The mild oxidation of nitrile oxide with NMO is compatible with the HDA route. Only minor amounts of the 1,3-dipolar cycloadducts derived from the competing cycloaddition of nitrile oxides to the dienes could be occasionally isolated. It is also compatible with the ene route, which works fine with tetra- and trisubstituted alkenes. Applications to the ene reactions are, however, less convenient with 1,2- and 1,1-disubstituted ethylenes and fail with monosubstituted ethylenes since an ene excess (> 10 equiv) is required in the ene route. Under these conditions the 1,3-dipolar cycloaddition heavily competes with the oxidation step of the nitrile oxides. The photochemical cleavage of **4** represents

the softest route to nitroso carbonyls and was applied to the first, and unique TR-IR detection of nitroso carbonyls by Toscano,⁹ through the laser photolysis of 1,2,4-oxadiazole-4-oxides **4** during his studies in the biological chemistry of nitrogen oxides. Moreover, photochemically generated nitroso carbonyls are fully compatible with the HDA and ene routes. They are easily trapped with differently substituted olefins affording the corresponding ene adducts in high yields because of the absence of any interfering reactions, aside from the nitroso carbonyl dimerization and the subsequent rearrangement of the fleeting dimers.^{8,10}

In studying the regioselectivity of the ene reactions of benzoyl nitroside (BN) and mesitoyl nitroside (MN) **7A,B** to a few trisubstituted olefins, we noted the intriguing changes of regioselectivity upon variation of the nitroso carbonyl substituent.¹¹ BN affords mainly the Markovnikov (M) adducts **9Aa–c**, in keeping with a prevailing frontier orbital (FO) interaction of the alkene HOMO with the nitroso carbonyl electrophilic nitrogen, while with MN comparable amounts of the M adducts **9Ba–c** and anti-Markovnikov (AM) adducts **10Ba** and (*E*)**10Bb,c** are formed (Scheme 2).

The ene reactions with the stereoisomeric (*E*)- and (*Z*)-3-methyl-2-pentenes **11E** and **11Z** allowed for the differentiations

(4) (a) Iwasa, S.; Tajima, K.; Tsushima, S.; Nishiyama, H. *Tetrahedron Lett.* **2001**, *42*, 5897–5899. (b) Flower, K. R.; Lightfoot, A. P.; Wan, H.; Whiting, A. *J. Chem. Soc., Perkin Trans. 1* **2002**, 2058–2064. (c) Iwasa, S.; Fakhruddin, A.; Tsukamoto, Y.; Kameyama, M.; Nishiyama, H. *Tetrahedron Lett.* **2002**, *43*, 6159–6161. (d) Pulacchini, S.; Sibbons, K. F.; Shastri, K.; Motevalli, M.; Watkinson, M.; Wan, H.; Whiting, A.; Lightfoot, A. P. *Dalton Trans.* **2003**, 2043–2052. (e) Adamo, M. F. A.; Bruschi, S. *J. Org. Chem.* **2007**, *72*, 2666–2669.

(5) Adam, W.; Bottke, N.; Krebs, O.; Saha-Möller, C. R. *Eur. J. Org. Chem.* **1999**, 1963–1965. (6) Keck, G. E.; Webb, R. R.; Yates, J. B. *Tetrahedron* **1981**, *37*, 4007–4016.

(7) (a) Quadrelli, P.; Mella, M.; Caramella, P. *Tetrahedron Lett.* **1998**, *39*, 3233–3236, and references therein. (b) Quadrelli, P.; Gamba Invernizzi, A.; Caramella, P. *Tetrahedron Lett.* **1996**, *37*, 1909–1996. (c) Quadrelli, P.; Mella, M.; Gamba Invernizzi, A.; Caramella, P. *Tetrahedron* **1999**, *55*, 10497–10510. (d) Quadrelli, P.; Mella, M.; Paganoni, P.; Caramella, P. *Eur. J. Org. Chem.* **2000**, 2613–2620. (e) Quadrelli, P.; Scrocchi, R.; Caramella, P.; Rescifina, A.; Piperno, A. *Tetrahedron* **2004**, *60*, 3643–3651. (f) Quadrelli, P.; Mella, M.; Carosso, S.; Bovio, B.; Caramella, P. *Eur. J. Org. Chem.* **2007**, 6003–6015. (g) Quadrelli, P.; Mella, M.; Assanelli, G. *Tetrahedron* **2007**, *64*, 7312–7317.

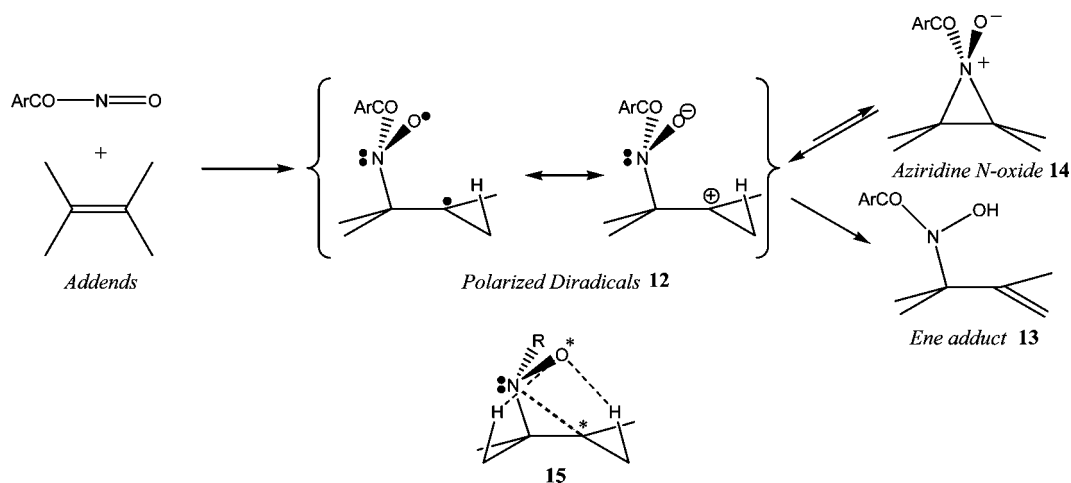
(8) (a) Quadrelli, P.; Mella, M.; Caramella, P. *Tetrahedron Lett.* **1999**, *40*, 797–800. (b) Quadrelli, P.; Campari, G.; Mella, M.; Caramella, P. *Tetrahedron Lett.* **2000**, *41*, 2019–2022.

(9) For recent direct observation of acyl nitroso species see: Cohen, A. D.; Zeng, B.-B.; King, S. B.; Toscano, J. P. *J. Am. Chem. Soc.* **2003**, *125*, 1444–1445.

(10) (a) Quadrelli, P.; Scrocchi, R.; Piccanello, A.; Caramella, P. *J. Comb. Chem.* **2005**, *7*, 887–892. (b) Quadrelli, P.; Caramella, P. *Curr. Org. Chem.* **2007**, *11*, 959–986.

(11) Quadrelli, P.; Mella, M.; Piccanello, A.; Romano, S.; Caramella, P. *J. Org. Chem.* **2007**, *72*, 1807–1810.

SCHEME 3



of the three possible stereochemical paths involved (Figure 1). The stereoisomeric enes **11E** and **11Z** have been extensively used in the investigations of ene reactions since they allow for fully defining the stereochemical paths and assessing the intriguing phenomenon known as the “cis effect.”¹² The cis effect typically occurs in singlet oxygen ene reactions and refers to the neat preference of singlet oxygen for the abstraction of the *twix* and *lone*¹³ allylic hydrogens from the more congested side of a trisubstituted olefin (Figure 1).

In the ene reactions of nitrosocarbonyls **7A,B** with the stereoisomeric enes **11E** and **11Z**, only the adducts deriving from the *cis* abstraction were observed.¹¹ BN **7A** afforded predominantly the adducts deriving from the *M* coupling of the nitrogen atom of the nitrosocarbonyl **7A** to the less substituted carbon of the olefin with abstraction of the *twix* hydrogens (dots in Figure 1). Only minor amounts of adducts were derived instead from an *AM* coupling of the nitrogen with abstraction of the *lone* hydrogens (squares). The experiments performed with MN **7B** and olefins **11E,Z** confirmed the neat *cis* effect, as well as the relief of *M* control characteristic of MN. In the case of the ene reaction with olefin **11E**, the *twix M* path is slightly prevalent over the *lone AM*, while the reverse holds for the ene reaction of olefin **11Z**. The results showed the remarkable and somehow unexpected *cis* selectivity of the ene reactions of nitrosocarbonyls as well as the noteworthy influence of the nitrosocarbonyl substituent on the regioselectivities, BN **7A** mainly giving the *M twix* adducts, while the bulkier MN **7B** afforded mixtures of *M twix* and *AM lone* adducts.

Model calculations¹¹ on the reaction of **7A,B** with tetramethylethylene (TME) gave insights on the origin of the relief of *M* selectivity with **7B**. The reaction takes place in a stepwise fashion with a rate-determining C–N bond formation of a formal

open-chain intermediate **12**, the so-called polarized diradical (PD),¹⁴ which readily rearranges to the ene adduct **13** by H transfer. Cyclization to the aziridine N-oxide (ANO) **14** is more difficult and reversible.

Using the terminology proposed by Singleton in the related triazolinedione (TAD) system,¹⁵ the ANOs behave as “innocent bystanders” in these reactions (Scheme 3).

At variance with the open-chain nature of these diradical intermediates, usually associated with a ready loss of stereochemical integrity due to easy bond rotations, Houk and Leach showed that the PDs **15** (R = H, Me, *p*-NO₂Ph) have to be viewed as unsymmetrically bonded intermediates with unexpectedly high (>4 kcal/mol) barriers of rotations around the single bonds of the N–C–C* moiety. Accurate analyses and CASSCF investigations, as well as validation of the use of DFT treatment by comparison with the best levels of theory available for systems of this size, provided the breakthrough and demonstrated that the PDs are resonance hybrids of diradical and zwitterionic structures.^{14b} The interactions between the two radical/zwitterionic sites lead to weak bonding between the nitroso nitrogen and trigonal carbon and weak O···H hydrogen bonds between the nitroso oxygen and the facing methyls, as shown by the dashed lines in **15**, thus restricting the otherwise easy bond rotations. Solvents were shown to affect the electronic structure of the hybrid PDs by decreasing the diradical contribution with increasing dielectric constant. Recently, Acevedo and Squillacote¹⁶ highlighted the role of solvent effects in the related ene reaction of 4-phenyl-TAD (PTAD) with TME and evidenced the zwitterionic nature of the open intermediate present in solution. The different solvations in aprotic and protic solvents accounted nicely for the reaction outcome with enes carrying

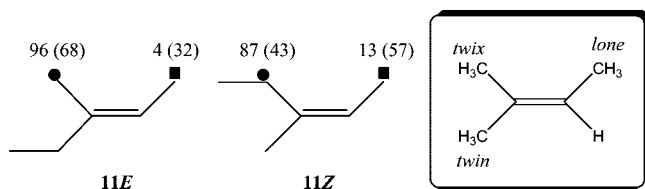


FIGURE 1. Percentage of hydrogen abstraction in the ene reactions of the stereoisomeric enes **11E** and **11Z** with BN **7A** and MN **7B** (in parentheses). The inset summarizes Adam's nomenclature for the reaction with trimethylethylene.¹³

(12) (a) Stephenson, L. M.; Grdina, M. J.; Orfanopoulos, M. *Acc. Chem. Res.* **1980**, *13*, 419–425. (b) Clennan, E. L. *Tetrahedron* **2000**, *56*, 9151–9179. (c) Stratakis, M.; Orfanopoulos, M. *Tetrahedron* **2000**, *56*, 1595–1615. (d) Leach, A. G.; Houk, K. N. *Chem. Commun.* **2002**, 1243–1255. (e) Singleton, D. A.; Hang, C.; Szymanski, M. J.; Meyer, M. P.; Leach, A. G.; Kuwata, K. T.; Chen, J. S.; Greer, A.; Foote, C. S.; Houk, K. N. *J. Am. Chem. Soc.* **2003**, *125*, 1319–1328.

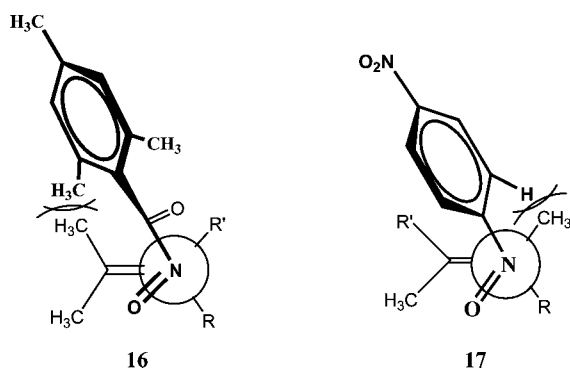
(13) For definition see: Adam, W.; Bottke, N.; Krebs, O. *J. Am. Chem. Soc.* **2000**, *122*, 6791–6792.

(14) (a) Leach, A. G.; Houk, K. N. *J. Am. Chem. Soc.* **2002**, *124*, 14820–14821. (b) Leach, A. G.; Houk, K. N. *Org. Biomol. Chem.* **2003**, *1*, 1389–1403.

(15) Singleton, D. A.; Hang, C. *J. Am. Chem. Soc.* **1999**, *121*, 11855–11893.

(16) Acevedo, O.; Squillacote, M. E. *J. Org. Chem.* **2008**, *73*, 912–922.

cyclopropyl substituents that were used as hypersensitive probes, to ascertain the occurrence of radical or zwitterionic intermediates.¹⁷



In the reactions of nitrosocarbonyls **7A,B** with TME, the transition structure (TS) of addition step **7A** to TME shows no special hindrance between the addends. The TS of **7B** shows that the mesityl group is twisted out of the nitrosocarbonyl plane, as usual, causing unfavorable steric crowding between its *ortho*-methyl and *trans*-distal TME methyl, as depicted in **16**. This crowding should slow down the M *twix* ($R = \text{Me}$, $R' = \text{H}$) and twin ($R = \text{H}$, $R' = \text{Me}$) approach of **7B** to a trisubstituted ethene and somewhat compensate the M electronic bias.

The related aromatic nitroso compounds ($\text{Ar}-\text{NO}$)¹⁸ in reactions with enes **11** show a distinctively dissimilar behavior instead giving exclusively M end selectivity with the *twix* abstraction favored over the twin. Model calculations of the reaction of 4- NO_2PhNO with TME indicated a reversible formation of the PD in this case, consistent with Houk's analysis^{14b} of available experimental results.^{18c} The TS of the addition step reveals a severe steric hindrance between an aryl-H and the *trans*-proximal TME methyl as depicted in **17**. This points out that the M *twin* ($R = \text{H}$, $R' = \text{Me}$) coupling of ArNOs with trisubstituted ethenes is sterically disfavored, while the AM lone ($R = \text{Me}$, $R' = \text{H}$) coupling is electronically and sterically disfavored.

We report a theoretical study on the ene reactions of nitrosocarbonyls **7A** and **7B** with trimethylethylene and (*E*)- and (*Z*)-3-methyl-2-pentenes **11E** and **11Z**, as well as a comparison of the addition TSs of the related ene reactions of 4- NO_2PhNO **7C**. The results confirm our previous interpretation, and document further the known inadequacy of B3LYP calculations, when rate-determining medium-range interactions are involved.

Methods

Geometries for all the stationary structures were optimized at the B3LYP level using the standard 6-31G* basis sets. The calculations were performed with the Gaussian 03 program.¹⁹ Diradical and transition states leading to diradicals were treated

with the unrestricted procedure, involving HOMO–LUMO mixing in the initial guess, leading to unrestricted wave functions. Restricted and unrestricted calculations yielded, however, identical structures for all species except for the PDs and few other cases specified in the text. All minima and transition states were characterized by their vibrational frequencies. All the reported thermodynamic data are given at 298.15 K from unscaled vibrational frequencies in the harmonic approximation. Intrinsic reaction coordinate (IRC) calculations starting at the saddle points were carried out to check the connections between the transition structures, reactants, and products. Solvent calculations were performed with the PCM-UAHF method.¹⁹ MPWB1K²⁰ calculations were performed with the recommended DIDZ [6-31+G(d,p)] basis.

Results and Discussion

B3LYP Free Energy Profiles of Nitrosocarbonyls with Trimethylethylene. Figure 2 shows the free energy profile of the ene reaction of BN **7A** and trimethylethylene **8a** leading to TSs, intermediates, and products **18A–24A**. In all the shown structures, the nitrosocarbonyl moiety is *transoid*. Cisoid structures, as exemplified in the inset for TS *cis*-**18Ax**, were also located, but their free energies were higher in energy by 2–5 kcal/mol and are not displayed.

The *twix* and *twin* M couplings of the addends (labeled *x* and *n*) are given on the left and are akin to the profile of the reaction of **7A** with TME.¹¹ Couplings take place through TSs **18Ax,n** to yield the corresponding PDs **19Ax,n**. The PDs easily undergo H-abstraction through TSs **20Ax,n** ending into the M adduct **21A(M)**. The PDs are also connected through the cyclization TSs **22Ax,n** to the higher lying ANOs **23A** *syn* and *anti*, where *syn* and *anti* indicate the relative position of the N–oxide oxygen and the disubstituted side of the aziridine C–C bond. The *syn* and *anti* ANOs **23A** exist in two different conformations, labeled “in” and “out” according to the relative locations of the carbonyl oxygen and less substituted aziridine carbon, and are linked through the rotation TSs **24A** *syn* and *anti*.

On the whole, the *twix* and *twin* M profiles indicate two consecutive reactions with the addition steps being rate- and product-determining, while the H-abstraction steps have small free energy barriers ($\Delta\Delta G^\ddagger = 1.8$ and 2.6 kcal/mol, respectively) of entropic origin. The H-abstraction barriers are determined by the higher order required in the TSs with respect to the PDs, and essentially disappear in the enthalpic profiles ($\Delta\Delta H^\ddagger = -0.2$ and 0.2 kcal/mol, respectively).

The PDs **19Ax,n** conform to the expectations for a polarized diradical as a resonance hybrid of diradical and zwitterionic structures. According to Houk's description,^{14b} unrestricted calculations suggest an approximate 1:1 weight of the diradical and zwitterionic structures in the *twix* ($\langle S^2 \rangle = 0.47$) and *twin* ($\langle S^2 \rangle = 0.59$) PD, while the restricted zwitterionic structures have quite similar geometries and lie at only slightly higher energies ($\Delta\Delta G = 0.9$ and 2.4 kcal/mol, respectively). Note, however, that in the case of the *twix* **19Ax**, the two structures are essentially equienergetic on the enthalpic ($\Delta\Delta H = 0.1$) and electronic ($\Delta\Delta E_{el} = 0.0$) profiles. The *twix* PD is more stable (by 2 kcal/mol) than the *twin* because of the two stabilizing $\text{NO}\cdots\text{H}-\text{CH}_2$ contacts and less steric hindrance of the benzoyl

(17) (a) Alberti, M. N.; Orfanopoulos, M. *Org. Lett.* **2008**, *10*, 2465–2468. (b) Roubelakis, M. M.; Vougioukalakis, G. C.; Angelis, Y. S.; Orfanopoulos, M. *Org. Lett.* **2006**, *8*, 39–42.

(18) (a) Adam, W.; Krebs, O. *Chem. Rev.* **2003**, *103*, 4131–4146. (b) Adam, W.; Krebs, O.; Orfanopoulos, M.; Stratakis, M. *J. Org. Chem.* **2002**, *67*, 8395–8399. (c) Adam, W.; Krebs, O.; Orfanopoulos, M.; Stratakis, M.; Vougioukalakis, G. C. *J. Org. Chem.* **2003**, *68*, 2420–2425. (d) Adam, W.; Botke, N.; Engels, B.; Krebs, O. *J. Am. Chem. Soc.* **2001**, *123*, 5542–5548.

(19) Frisch, M. J.; et al. *Gaussian 98, Revision A.9*; Gaussian, Inc.: Pittsburgh, PA, 1998, and *Gaussian 03, Revision B. 02*; Gaussian, Inc.: Pittsburgh, PA, 2003.

(20) (a) Zhao, Y.; Truhlar, D. G. *J. Phys. Chem. A* **2004**, *108*, 6908–6918. (b) Zhao, Y.; Truhlar, D. G. *Acc. Chem. Res.* **2008**, *41*, 157–167.

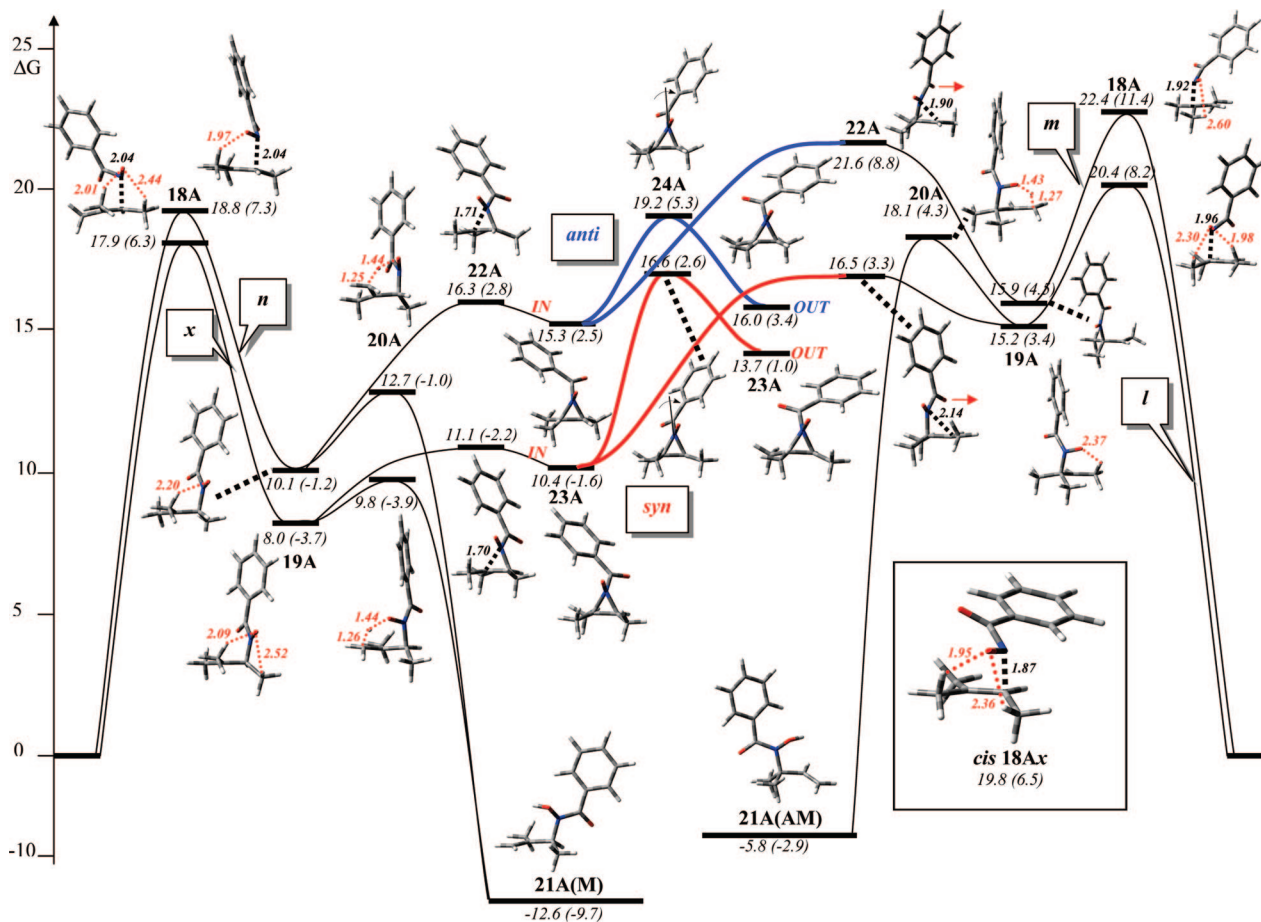


FIGURE 2. Free energy profile of the ene reaction of BN **7A** and trimethylethylene **8a**. Numbers near the levels show free energies (enthalpies in parentheses) in kcal/mol relative to the reactants. In the formulas the NO oxygen points toward the observer, dashed lines in TSs indicate N–C bond formation, and the red dotted lines specify the NO \cdots HC contacts. Numbers near formulas specify relevant bond distances in Å.

substituent located in the less encumbered trans space. The same applies at varying degrees to all the structures of the *x* and *n* profiles, as well as to the syn and anti ANOs. The preference for the “in” conformation over the “out” in the ANOs **23** can be related to the better donor character of the more substituted C–N ANO bond, which eclipses the $p_z \pi^*_{CO}$, as reported for the related N-acyl aziridines.²¹

The profiles of the AM couplings are lifted and show a feasible interconversion of the PDs. On the right of the Figure 2, the TS **18AI** and the unrestricted TS **18Am** ($\langle S^2 \rangle = 0.31$; the restricted TS is 1.5 kcal/mol above) are depicted leading to the AM PDs, **19AI** and **19Am**. The latter is a diastereoisomer of **19AI** where the β -methyl on the N-oxide oxygen side is missing (*m*). The AM PDs rise sizably in energy with respect to the M ones owing to the less stabilization of a secondary radical and even lesser stabilization of a secondary carbocation. The diradical character, thus, increases in **19AI** ($\langle S^2 \rangle = 0.71$) and becomes prominent in **19Am** ($\langle S^2 \rangle = 0.85$). The restricted structure **19Am** lies 6.3 kcal/mol above while the restricted **19AI** does not have a stable minimum. In the case of the lone PD **19AI**, the H-abstraction barrier is still low ($\Delta\Delta G^\ddagger = 2.9$, $\Delta\Delta H^\ddagger = 0.9$ kcal/mol), but the cyclization barrier **22AI** (unrestricted, $\langle S^2 \rangle = 0.26$) is a little lower ($\Delta\Delta G^\ddagger = 1.3$, $\Delta\Delta H^\ddagger = -0.1$ kcal/mol), making cyclization slightly preferred over H-abstraction. Cyclization leads (IRC) to the ANO **23Asyn-in** since in the closure the carbonyl group moves away from (arrow) the facing ternary methyl. The AM lone profile shows then a feasible competing route for the conversion of the initially formed PD

19AI to PD **19Ax** through the syn ANO. Diradical **19m** is the highest in energy among the PDs and can hardly be a significant intermediate in these reactions. It has no available direct H-abstraction route and lies in a deep minimum. It should conceivably undergo bond rotation to **19AI** because of its increased diradical character or cyclize through the high barrier **22Am** to the ANO **23Aanti-in** and then rearrange to the twin PD **19Ax**, finally yielding the adduct **21A(M)**.

Clearly, the formation of the ene adducts **21A(AM)** is disfavored either by the higher TSs of the AM couplings or by the possible competing rearrangements of the AM PDs **19AI,m** to the M ones. Routes to **21A(AM)** could be somewhat improved by hindering the rearrangements of the PDs, e.g., by destabilization of the ANOs with concomitant increases of the cyclization barriers leading to them. This applies well in the case of the bulky mesityl substituents of **7B**. Moreover, as already discussed (cf. **16**), the steric clashes between mesityl substituent and geminal methyls of trimethylethylene **8a** should raise the energy of the addition TSs of both the twix and twin M paths. Calculations were performed on the ene reaction of MN **7B** and **8a** by using the 2,6-dimethylphenyl in the place of the mesityl substituent. The profile leading to TSs and inter-

(21) (a) Shustov, G. V.; Kadorkina, G. K.; Varlamov, S. M.; Kachanov, A. V.; Kostyanovsky, R. G.; Rauk, A. *J. Am. Chem. Soc.* **1992**, *114*, 1616–1623. (b) Mimura, N.; Miwa, Y.; Ibuka, T. *J. Org. Chem.* **2002**, *67*, 5796–5801. (c) Otani, Y.; Nagae, O.; Naruse, Y.; Inagaki, S.; Ohno, M.; Yamaguchi, K.; Yamamoto, G.; Uchiyama, M.; Ohwada, T. *J. Am. Chem. Soc.* **2003**, *125*, 15191–15199. (d) Alkorta, I.; Cattivela, C.; Elguero, J.; Gil, A. M.; Jemenez, A. I. *New J. Chem.* **2005**, *29*, 1450–1453.

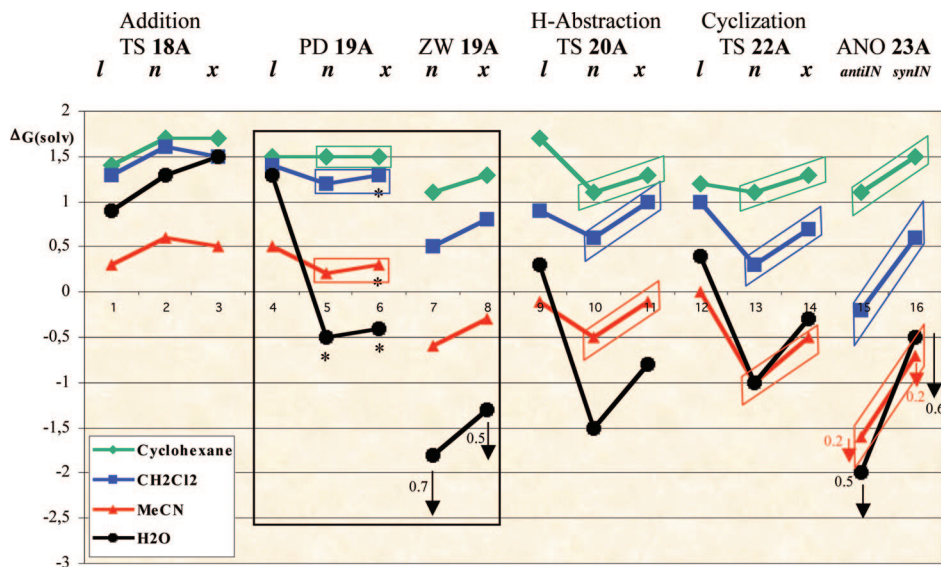


FIGURE 3. Free energy corrections $\Delta G(\text{solvent})$ in kcal/mol calculated on the gas-phase structures of the relevant addition TSs **18A**, PDs and ZWs **19A**, and ANOs **23A**. The downward arrows specify optimizations in solvents that give an additional energy gain larger than 0.1 kcal/mol. Cases with an asterisk are discussed in the text.

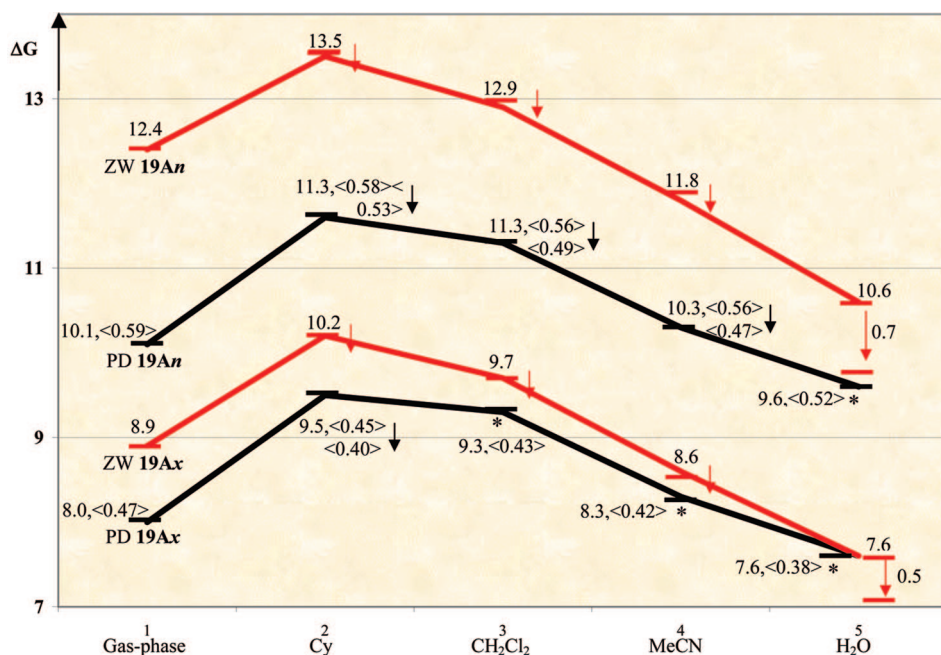


FIGURE 4. Effect of solvation on the relative free energies (kcal/mol) and $\langle S^2 \rangle$ values of PDs and ZWs **19n,x**. Downward arrows and asterisks have the same meaning as in Figure 3.

mediates **18B–23B** is given in the Supporting Information (SI). At variance with expectations, the addition and abstraction steps look akin to those of BN **7A** and only the spacings between the TSs **18B** decrease somewhat (vide infra). The presence of the bulkier substituent increases the crowding in the ANOs and raises their energy well above the H-abstraction barriers, thus offsetting possible diradical interconversions through the ANOs.

Solvent Effects. Solvents may affect the gas-phase profile discussed above by differential solvation of the reactants, TSs, intermediates, adducts and by modifying the mechanism and roles of the PD and ANO intermediates. Figure 3 summarizes the effect of four solvents of increasing dielectric constants (cyclohexane, methylene chloride, acetonitrile, and water) on the relevant structures and shows the $\Delta G(\text{solvents})$ corrections relative to the reactants as obtained with PCM-HAHF single-

point calculations on gas-phase geometries. Optimizations in solvent have been performed for the addition TSs **18A**, PDs and ZWs **19A**, and the ANOs **23A**. The additional energy gain is given near the downward arrows when relevant (>0.1 kcal/mol). The four points labeled with an asterisk are discussed in the text.

The cyclohexane green lines on the top cluster around 1.4 ± 0.3 kcal/mol and point to a rather uniform solvent effect on the various structures less solvated than the reactants. The spread of the points becomes more visible in the methylene chloride series (blue lines), increases in acetonitrile (red lines), and even more in water (black lines) where deviations of up to ± 2 kcal/mol occur. As expected, the polar ANOs are remarkably stabilized with respect to the PDs, but not enough to fully compensate the greater gas-phase stabilities of the PDs. Looking

TABLE 1. Relative Free Energies^a (Electronic Energies) of TSs 18A–C^b

TS	B3LYP	MPWB1K/B3LYP	Δ^c	$\Delta_{\text{twin}}^{c,d}$
18Ax	0 (0)	0 (0)	0	-1.1
18An	0.9 (1.0)	2.0 (2.1)	1.1	0
18Al	2.5 (2.0)	1.6 (1.1)	-0.9	-2.0
18Bx	0 (0)	0 (0.5)	0	-0.3
18Bn	0.4 (0.4)	0.7 (1.2)	0.3	0
18Bl	1.3 (0.8)	0 (0)	-1.3	-1.6
18Cx	0 (0)	0 (0.0)	0	0.3
18Cn	1.9 (2.2)	1.6 (1.9)	-0.3	0
18Cl	4.7 (4.3)	3.3 (2.9)	-1.4	-1.1

^a In Kcal/mol, free energies at 298.15 K. ^b In TSs **18B** the mesityl was replaced by 2,6-dimethylphenyl in the calculations. ^c Difference between the relative MPWB1K and B3LYP free energies. ^d Free energy changes relative to TS **18A–Cn**.

at the bars in Figure 3, which evidence the structures related to the twin and twix profiles, it is easy to see that the solvent stabilization increases in the order PDs < H-abstraction TSs < cyclization TSs < ANOs in all cases except for water.

In the aprotic solvents the increasing polarity of the solvent enforces the PD minima to become more shallow and the ANO minima more deep while cyclizations (equilibrations of the PD with the ANOs) are incremented over H-abstractions. A similar trend was noted by Acevedo and Squillacote in a study of the PTAD/TME system in apolar solvents which accounted for the lack of rearrangements of cyclopropyl hypersensitive probes. The latter, however, rearrange in protic solvents¹⁷ because of a change in the nature and stability of the PD intermediates which turn into true zwitterions.¹⁶

The same applies to our system. In water the ZWs **19n,x** are remarkably stabilized, just as the ANOs, and may drop energetically below the PDs, becoming the true intermediates in these reactions. Figure 4 displays the effect of solvation on the free energy of PDs and ZWs **19n,x**. The reported ΔG values and $\langle S^2 \rangle$ values refer to single-point calculations while downward arrows specify optimizations in solvent yielding a lower $\langle S^2 \rangle$ and an energy gain which is given when larger than 0.1 kcal/mol. The figure shows that a switch of free energy of the twix ZW/PD **19Ax** couple occurs in water while the twin ZW **19An** still remains above the PD, even if by only a negligible amount. The PD levels marked with an asterisk indicate cases where optimizations in solvent led to the corresponding and, in most cases, higher lying ZWs. These, at first, surprising results can be understood since optimizations run in Gaussian on the electronic surface where negligible (in the *twix* case) or small (0.5 kcal/mol for the *twin* case) electronic energy differences exist in the ZW/PD couples. The optimization outcome is driven by the electronic energy only. As a matter of fact, the energies (electronic and free) of PDs and ZWs are close in these cases, and the present calculations foster the PDs on the free energy surface in all cases except for **19Ax** in water.

In summary, aprotic solvents do not change sizably the mechanism implied in the gas-phase profile. In the case of water, an interesting change in the nature of the lowest unsymmetrical bonded intermediate is predicted, opening the possibility of trapping the zwitterionic intermediate by enhancing the cation stabilization with appropriate structural modifications. As far as the addition TSs are concerned, apolar solvents cause a slight promotion (by 0.3 kcal/mol) of the lone additions over the twin and twix ones, and optimizations in solvents do not sizably change the trend.

Medium Range Effects. The B3LYP profiles provide a detailed knowledge of the elementary steps involved in the nitrosocarbonyl ene reactions and sound support for a two-step mechanism where the addition steps are rate- and product-determining. On the other hand, the calculated addition barriers steadily increase in the order *twix* < *twin* < *lone* and do not fit the experimental results. Actually, the calculated addition barriers do not reproduce either the observed cis effect of **7A,B** (TSs **18A,B** *twin* the highest) or the relief of M selectivity of **7B** (TS **18B** *twix* ~ *lone*). This could be due to a known deficiency of B3LYP calculations since conventional functionals neglect medium-range electron correlation effects (a “theoretical disaster”, in the words of ref 22). Therefore, they are unable to deal with weakly bound molecular complexes and structures where dispersion forces are critical.²³ New families of functionals have been, however, developed to deal with the medium range effects and, in particular those developed by the Truhlar group, perform satisfactorily in several cases.²⁰

Upon using the recommended MPWB1K functional,^{20a} the picture improves considerably (Table 1). The table compares the relative free energy barriers of TSs **18A,B** as obtained by the B3LYP optimizations and the MPWB1K/6-31+G**//B3LYP calculations by using the B3LYP geometries and vibrational corrections. Related functionals (MPW1K, MPW1B95)²⁰ give values of relative electronic energies similar to those obtained with the MPWB1K.

At the MPWB1K level the twin TSs **18An** and **18Bn** gratifyingly become the highest barriers, in keeping with the observed cis effect of **7A** and **7B**. In the case of **7A**, TS **18Ax** is sizably favored over TS **18Al**. In the case of **7B**, TSs **18Bx** and **18Bl** are almost equienergetic, in keeping with the characteristic relief of M control with the mesityl derivative. The fourth column (Δ) of Table 1 gives the changes of the free energies from B3LYP to MPWB1K and is attributable to the medium-range effects. The changes are reordered in the fifth column (Δ_{twin}) with reference to the trans twin TSs to better evidence the stabilization of the cis TS **18Ax** and **18Al**. Admittedly, partitioning of the medium range effects among attractive van der Waals (vdW), electrostatic, and repulsive (Pauli) interactions is quite a difficult task.²² However, one can take into account the essential role of (intramolecular) vdW interactions in accounting for alkane thermochemistry^{22,23} as well as the (intermolecular) vdW interaction in the textbook explanation of the bp differences between branched and normal alkanes. Thus, in the search for a simple, yet sensible physical model, it is tempting to attribute the different Δ_{twin} stabilization of the cis TSs **18Ax** and **18Al** to the additional cis NO \cdots HC electrostatic contacts present in both cases and the wider dispersive vdW contacts in the lone one.²⁴ In the mesityl case, the stabilization still takes place in TS **18Bl**, but it is almost relieved in TS **18Bx** because of the opposing *ortho*-methyl–methyl (Pauli) clash.

Also given in the table are the relative free energies of the addition TSs **18Cx,n,l** of the related reactions of 4-NO₂Ph-NO

(22) Grimme, S. *Angew. Chem., Int. Ed.* **2006**, *45*, 4460–4464.

(23) (a) Schreiner, P. R. *Angew. Chem., Int. Ed.* **2007**, *46*, 4217–4219. (b) Schwabe, T.; Grimme, S. *Phys. Chem. Chem. Phys.* **2007**, *9*, 3397–3406. (c) Wodrich, M. D.; Wannere, C. S.; Mo, Y.; Jarowski, P. D.; Houk, K. N.; von Ragué Schleyer, P. *Chem. Eur. J.* **2007**, *13*, 7731–7744. (d) Wodrich, M. D.; Corminboeuf, C.; Schreiner, P. R.; Fokin, A. A.; von Ragué Schleyer, P. *Org. Lett.* **2007**, *9*, 1851–1854.

(24) For an interesting case of vdW steric attraction in a TS see: (a) Suarez, D.; Sordo, J. A.; Sordo, T. L. *J. Phys. Chem.* **1996**, *100*, 13462–13465. (b) Neureiter, N. P. *J. Am. Chem. Soc.* **1966**, *88*, 558–564.

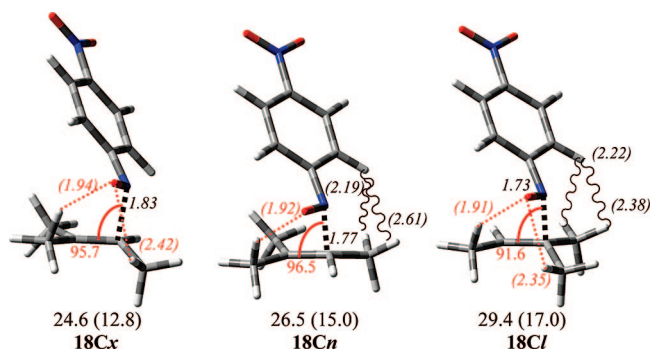


FIGURE 5. Side view of the B3LYP/6-31G* TSs **18Cx,n,l**. Activation free energies (enthalpies) are given in kcal/mol. Bond distances are in Å. The CH...O contacts (dotted) and steric clashes (wavy lines) are shown in parentheses. The attacking NCC angles are shown in red.

TABLE 2. Distortion Energies of Ene **8a**, Enophiles **7A–C**, and Total in TSs **18A–C**^a

TS	Ene	Enophile	Total
18Ax	7.9 (≡0.0)	6.9 (≡0.0)	14.8 (≡0.0)
18An	9.6 (1.7)	6.7 (−0.2)	16.3 (1.5)
18Al	9.1 (1.2)	8.1 (1.2)	17.2 (2.4)
18Bx	8.2 (≡0.0)	6.3 (≡0.0)	14.5 (≡0.0)
18Bn	9.3 (1.1)	5.8 (−0.5)	15.1 (0.6)
18Bl	9.5 (1.3)	6.6 (0.3)	16.1 (1.6)
18Cx	13.5 (≡0.0)	2.7 (≡0.0)	16.2 (≡0.0)
18Cn	14.3 (0.8)	3.4 (0.7)	17.7 (1.5)
18Cl	17.7 (4.2)	4.3 (1.6)	22.0 (5.8)

^a B3LYP calculations are in kcal/mol. The numbers in parentheses are relative distortion energies.

7C with trimethylethylene **8a**. The gaps between the TSs are remarkably amplified, and the relatively weaker medium range effects (Δ twin) do not sizably change the B3LYP TS ordering.

The ordering of the TSs **18C** corresponds to the well-documented twix > twin \gg lone selectivity^{18d} and can be accounted for within the simple steric model shown in **17** by a combination of destabilizing steric (in TSs twin and lone) and electronic (disfavoring the AM lone) effects. The TSs **18Cx,n,l** are shown in Figure 5. As already noted, for the ene reaction with TME,¹¹ the TSs of **7C** are late with respect to the corresponding TSs of **7A,B**. The forming C–N bonds of the latter are around 2.0 Å and shorten to 1.83, 1.77, and 1.73 Å in TSs **18Cx,n,l**, respectively, while the activation parameters increase by 6.5–9.0 kcal/mol to the values reported in the figure.

Owing to the later character of the TSs **18C** with respect to TSs **18A,B**, an increasing role of the factors which stabilize the primary adducts (the PDs) is then expected, implying an increasing role of the distortion energies (DEs) of the addends in the ene reactions of **7C**. The role of DE in affecting reactivity has been frequently discussed in the framework of Morokuma's energy decomposition analysis,²⁵ and an earlier qualitative application of DEs in accounting for reactivity and selectivity trends in ene reactions has been reported.^{25c} In short, the activation barrier ΔE^\ddagger of a bimolecular reaction is partitioned according to the simple equation $\Delta E^\ddagger = \text{DE} + \text{INT}$. DE is the energy required to distort the

addends into the geometry in the TSs, and INT is the remaining part of ΔE^\ddagger that takes into account the interaction energy between the distorted addends. In selectivity problems $\Delta\Delta E^\ddagger = \Delta\text{DE} + \Delta\text{INT}$ and two limiting cases can be envisaged, i.e., DE-controlled reactions (late TSs) when $\Delta\text{DE} \gg \Delta\text{INT}$ and INT-controlled reactions (early TSs) in the opposite case. A thorough application of the DE/INT model to 1,3-dipolar cycloadditions has recently appeared.²⁶

The DEs of the addends in the TSs of the ene reactions of trimethylethylene **8a** with enophiles **7A–C** are gathered in Table 2. The figures show that in the reactions of nitroso-carbonyls **7A,B**, the DEs of ene **8a** do not differ greatly and are only slightly larger than those of the enophiles **7A,B**. The total DEs differ by less than 2.4 and 1.6 kcal/mol in TSs **18A,B**, respectively. Their influence on the barrier heights can be readily overcome by the contributors to the interaction energy, i.e., the familiar terms of the Klopman–Salem equation,²⁷ such as FO interactions, closed-shell repulsions, and coulombic effects.

On going to the late TSs **18C**, the role of the DEs of the ene increases remarkably with respect to that of the enophile **7C**. Moreover, the DEs in the lone AM TS **18Cl** are remarkably higher than those of the M TSs **18Cx,n**. Thus, the total value of the DE of the lone is about 5 kcal/mol above the twix and twin and is no more easily modifiable by the contributors to the interaction energy. In summary, the late TSs of the ene reactions of ArNOs heavily depend on the DEs of the enes which enforces the M bias.

Selectivities with (E)- and (Z)-3-Methyl-2-pentenes 11. We have located the TSs **25** and **26** of the enophiles **7A–C** ene reactions with the stereoisomeric enes **11E** and **11Z**. The results are summarized in Figure 6. The location of the additional methyl on the trimethylethylene skeleton is indicated as anti (a), in (i) or out (o). The CH bond facing the NO oxygen is always rotated toward the oxygen to gain the CH...O (dotted) stabilizing interaction with a C=C–C–H dihedral angle of about 60°.

The labeled methyls bound to the olefinic carbon undergoing attack always stagger the forming C–N bond, as shown in the lone TSs. The other two labeled methyls in TS **25x** and **26n** adopt varying conformations depending upon the requirements of the TSs. In the reactions of **7C** the C-*i* eclipses the C=C bond as shown, while in the reactions of **7A,B** CH-*i* is rotated anticlockwise to recover the (weak) CH...O=C contacts.

The MPWB1K/B3LYP relative free energies have been obtained in the same fashion as those in Table 1 and are reported near the locations of the methyl substituent. Also shown are the Boltzmann % contributions of the various TSs to adduct formation assuming a rate- and product-determining addition. Significant contributions (>10%) are shown in bold red.

With ene **11E**, the TSs **25A–Cx** anti are the lowest and afford the largest amounts of ene adduct, along with minor contribution of the in and (in the case of **7A**) out paths. The out TSs **25B,Cx** are increased by 2.0 and 1.8 kcal/mol because of the severe steric crowding shown in Figure 7. In the mesityl case **7B**, the anti and in TS **25Bx** are also destabilized by the *ortho*-methyl–methyl clash, allowing for competition of TSs **25Bl** anti and out.

(26) (a) Ess, D. H.; Houk, K. N. *J. Am. Chem. Soc.* **2007**, *129*, 10646–10647. (b) Ess, D. H.; Houk, K. N. *J. Am. Chem. Soc.* **2008**, *130*, 10187–10198.

(27) (a) Fleming, I. *Frontier Orbitals and Organic Chemical Reactions*; Wiley, J. and Sons: London, UK, 1976; p 27. (b) Klopman, G. *J. Am. Chem. Soc.* **1968**, *90*, 223–234. (c) Salem, L. *J. Am. Chem. Soc.* **1968**, *90*, 543–566.

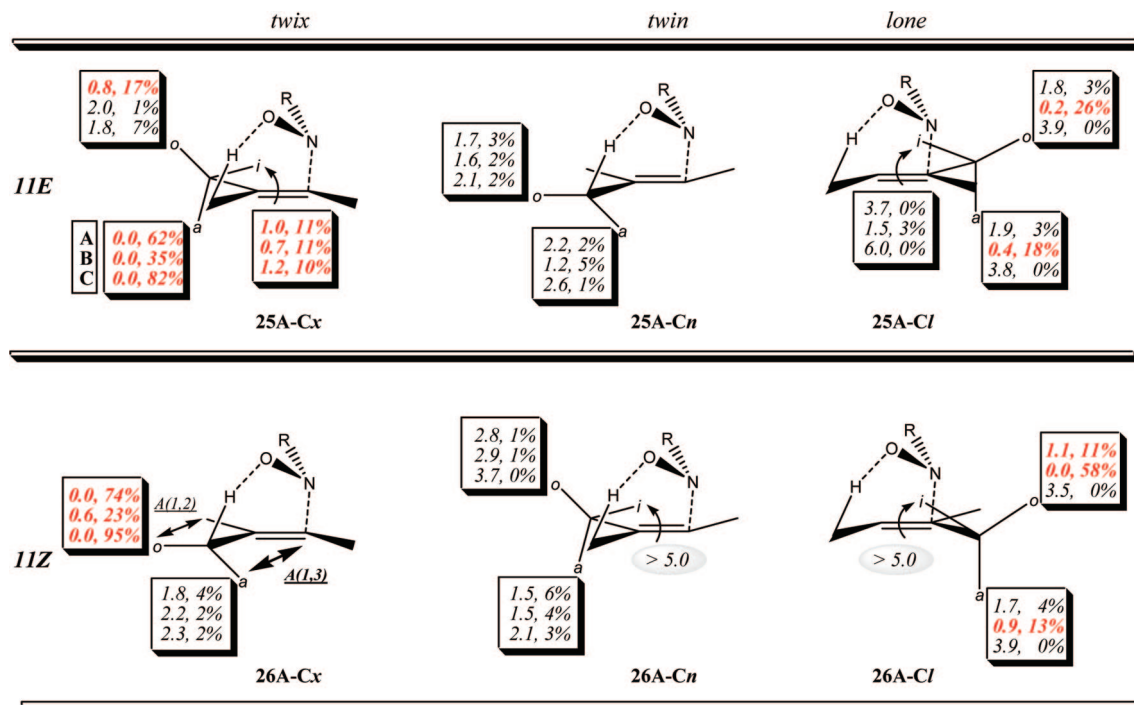


FIGURE 6. Selectivity in the ene reactions of enes **11E,Z** with enophiles **7A–C**. Numbers in boxes are relative MPWB1K/B3LYP free energies in kcal/mol and % contribution to adduct formation.

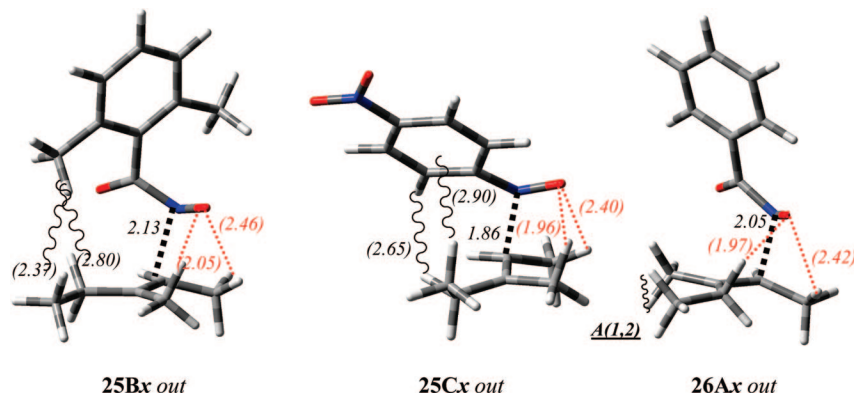


FIGURE 7. Hindrance in TS **25Bx out** and **25Cx out** and A(1,2) strain in TS **26Ax out**.

TABLE 3. Calculated (Experimental in Parentheses) Distribution of the Ene Adducts in the Ene Reactions of Enes **8a** and **11E,Z** with Enophiles **7A–C**

enes	enophiles	twix:twin:lone
8a	7A	90: 3: 6
	7B	43: 13: 43
	7C	93: 6: 0.4
11E	7A	89: 5: 5 (96: 0: 4) ^a
	7B	47: 7: 46 (68: 0: 32) ^a
	7C	97: 2: 0 (100: 0: 0) ^b
11Z	7A	78: 7: 15 (87: 0: 13) ^a
	7B	24: 5: 71 (43: 0: 57) ^a
	7C	97: 3: 0 (70: 30: 0) ^b

^a Reaction in CH₂Cl₂ at rt (ref 11). ^b Reaction in CDCl₃ at 0 °C (ref 15).

With ene **11Z** the TSs **26A–Cx** suffer by a large A(1,3) strain in the anti (bold double arrow) or by A(1,2) strain²⁸ in the out (double arrow) allowing for increasing competition

of the less encumbered lone TSs **26A–CI out**. The out TSs **26A,Cx** remain, however, the lowest paths for **7A,C**. In the case of the mesityl derivative **7B**, the additional *ortho*-methyl–methyl clash lifts the out path above the less encumbered TS **26BI out**, switching the selectivity to the AM side.

The calculated distributions of the adducts are compared with the experimental data in Table 3. In our opinion, the agreement is good for the reaction of nitrosocarbonyls **7A,B**. The decrease of the twix adducts from **11E** to **11Z** is well reproduced and attributable to the A(1,3) and A(1,2) strain.

The results for the ArNO **7C** obtained under the named assumptions (addition as limiting step) are less satisfactory, but the agreement can be improved significantly by taking into account the variable reversibility of the addition step of ArNOs.^{18c} As already suggested by Adam,^{18d} reversibility should be more important in the primary adducts deriving

(28) Hoffmann, R. W. *Chem. Rev.* **1989**, *89*, 1841–1860.

from the twix addition to **11Z** because of the destabilizing A(1,2) strain and lead to a decrease of the yield of the twix adducts.

Conclusions

Nitrosocarbonyls are fleeting and highly reactive intermediates which undergo ene reactions in a two-step fashion. The addition steps are rate- and product-determining and lead to polarized diradicals that readily enter the H-abstraction steps to yield the ene products. The addition TSs are early, and the stabilizing CH \cdots O contacts drive the reactions to the cis twix and lone adducts. The twix M path is prevailing in the case of BN **7A**, but steric effects compensate the electronic M bias in the reaction of the mesityl derivative **7B**. Aprotic solvents do not sizably change the gas-phase profile, but protic solvents may change the nature of the intermediates. B3LYP calculations alone do not describe the correct ordering of addition TSs in the ene reaction with trimethylethylene, and only at the MPWB1K level the medium-range noncovalent interactions involved are successfully recovered.

The more stable and isolable ArNOs exhibit late TSs in their ene reactions. The distortion energy becomes dominant and drives the reaction exclusively to the M adducts. The

twix adducts are favored over the twin mainly because of steric effects hindering the twin approach.

The addition TSs of the ene reaction of nitrosocarbonyls **7A,B** to the (*E*)- and (*Z*)-3-methyl-2-pentenes **11E** and **11Z** satisfactorily account for the experimental selectivities and evidence the origin of the decreasing twix preference of **11Z**. In the reactions of **11Z** the twix TS anti is severely hindered by the A(1,3) strain, while the TS out is also somewhat destabilized by the A(1,2) strain, allowing for competition of the less encumbered lone TS. In the case of ArNO **7C**, the agreement looks poorer but is understandable in terms of the variable reversibility of the addition steps of ArNOs.

Acknowledgment. Allocations of computer time by the Computer Centre of Pavia University and CILEA as well as by CINECA are gratefully acknowledged. Financial support by University of Pavia and Ministero dell'Università e Ricerca (MiUR: PRIN 2005) is also gratefully acknowledged.

Supporting Information Available: Free energy profile of the ene reaction of BN **7B** and trimethylethylene **8a**, full quotation of ref 19 for Gaussian 98 and 03, Cartesian coordinates, and thermodynamic data of reactants and TSs. This material is available free of charge via the Internet at <http://pubs.acs.org>.

JO801641J